

Influence of Diesel Fuel Properties on Atomization Characteristics

Authors- Syamantak Bera (11941220) , Vatsalya Meena(11941320)

Abstract:

This paper studies the influence of diesel fuel properties of Diesel, 50 percent mix of diesel and kerosene, and detergent type additive mixed with diesel on the atomization characteristics by PDA measurement in both quiescent and crossflow conditions. The spray pulsed data and the time-resolved data were studied in each case. SMD (Sauter Mean Diameter), drop size distributions, and drop velocities were studied. Along with PDA measurements were done for three different types of fuels Dimethyl ether, Diesel, and biodiesel, and their SMD and frequency distributions were studied. In first setup The diesel, 50- percent blend with kerosene and additized diesel had very less influence on the size of the droplets, with variances of smaller than $3\mu\text{m}$ (15 percent). A narrow spray (cone angle lesser than 20%) was observed in The diesel-with additive fuel than either the diesel fuel or the diesel blended with kerosene. Also in second setup Biodiesel and diesel fuels have an SMD range of 30-70 metres, whereas DME fuel has an SMD range of 10-40 metres. As of the volatility of DME is more and density is less , its atomization performance is superior than diesel fuels and biodiesel, according to these findings. Thus combining the two setups result obtained indicated that there was no significant effect on the size of the droplet due to the change in diesel fuels, though there were changes in the spray cone for additives mixed diesel. However for Dimethyl Ether due to high volatility, low surface tension, and low viscosity atomization was more.

INTRODUCTION:

Rapid industrialization has led to an increase in the use of gasoline and diesel engines. It is important to efficiently increase the performance of the diesel engine. Efficiency can be improved in two ways one by reducing the exhaust emissions of carbon monoxide, unburnt carbon, and nitrogen oxides and improving the thermal efficiency of the engine. There have been several studies on improving the performance of the engine some of which focuses on the spray characteristics of the engine. Atomization plays an important role in the spray characteristics along with the cone angle and penetration. In order for better efficiency and reducing exhaust emissions, atomization performance can be improved. Among several ways, one can be by changing the diesel fuel. Fuel atomization is improved by increasing the pressure during injection. Thus it can be assumed that the smaller droplet size can give better performance by reducing the emissions. Thus it is important to understand the influence of diesel fuel properties on the atomization characteristics.

There have been several studies on diesel sprays using the Phase Doppler Anemometry [8,9,10] but still, data sample sizes are limited. There is much scope for improvement and thus this study focuses on the results that can be obtained by using PDA techniques on different fuels and studying their atomization behaviors, a bit of spray cone characteristics too. The paper focuses on PDA and droplet measuring system to measure the droplet size and there variations with the change of fuel characteristics. The droplet size-frequency distribution, SMD, and mean velocity of the droplets were also measured. Normal production diesel, a 50 percent blend of diesel and kerosene, and diesel mixed with a detergent type polar additive was used in one experiment. The other experiment focussed on 3 different types of fuels. One industrial diesel, another biodiesel as it has similar properties as that of diesel and an alternative Dimethyl Ether. DME has different densities and surface tension from that of diesel in terms of density, viscosity, and surface tension. Thus it would help to build a clear picture of how density, viscosity, or surface tension of fuels can bring about change in the atomization characteristics. The spray cone characteristics, SMD characteristic, the axial- radial distance, and droplet distribution were studied. Though there are techniques where computer models [11,12,13,14] are used to get the atomization characteristics PDA can record the speed and size of high-speed droplets thus we use it for our study. From the available articles and theories, [1,2,3,4] it is evident that a change in fuel density or viscosity brings changes in droplet size, penetration.

EXPERIMENTAL SETUP 1 :

Fuels:

Diesel fuels density range is relatively narrow, for example, the CEN EN590 specification specifies density in 822-862 kg/m³; a difference of less than 5%. Nonetheless, changes in emissions have been seen in the EN590 range as a result of altering fuel characteristics, and it is possible that some of this effect is due to fuel effects on spray production.[5]

Base fuel impacts were investigated in this study using diesel fuel, a 50 percent mixture of kerosene and diesel fuel mixed with additives,. For many years Polar detergent additives, which could have surface effects on the fuel might affect the spray formation have been used.

A treat rate of two Thousand ppm was employed to explore any impacts of detergent-type additives, which is significantly greater than normal .

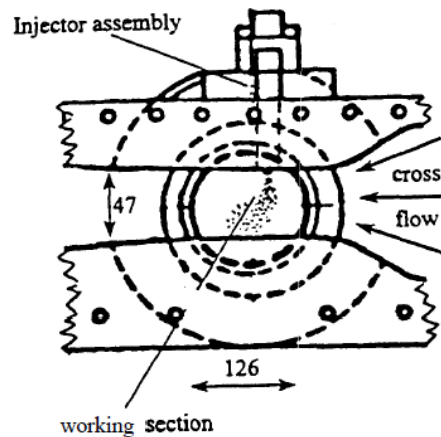


Fig 1 Working section region of High Pressure and Temperature Windtunnel.

Table 1: Fuels studied

Fuel	Density (kg/m ³)	Viscosity (cSt; 40°C)	Refractive Index (20°C)
European Diesel	850.9	3.15	1.476
50/50 Diesel / kerosene	828.4	1.93	1.463
Diesel + additive (2000 ppm)	850.9	3.13	1.476

High-Pressure Windtunnel:

As described in earlier papers, [6] fuel was pumped in using an injector which was held vertically into a wind tunnel keeping the pressure high, to investigate fuel impacts on the atomization process. Figure 1 demonstrates the wind tunnel, which had measurements of 47-millimeters, 120-millimeter width, and 126-millimeter length. For viewing the working section, two highly polished quartz windows were placed opposite each other. The wind tunnel provided both cross-flow of gas and a quiescent gas. The crossflow gas was monitored at 12m/s using the PDA. The goal of this research was to look at the atomization process. To suppress fuel ignition and vaporization, the fuels were injected at ambient pressure and temperature (14 bar CO₂ , 21°C) at a density near-normal Diesel.

Fuel Injector:

A sac-type injector was used, with one 200µm hole at the center. A 4 cylinder injection pump injected 4.4mm³ of fuel in the fuel injection system for each pulse. . With the highest injection pressure of thirty-seven Pascal, the pressure was set at twenty-two MegaPascal for the needle. The injector was chosen similar to research at Princeton University[7]. The time it took for the needle to open was one ms. At TDC, one synchronization pulse from the motor of the pump was employed after each phase was complete, to synchronize injections. A maximum of 7.2ms temporal frame surrounding the injecting pulse was created with a pulse generator on the processor (signal), as shown in Figure 2.

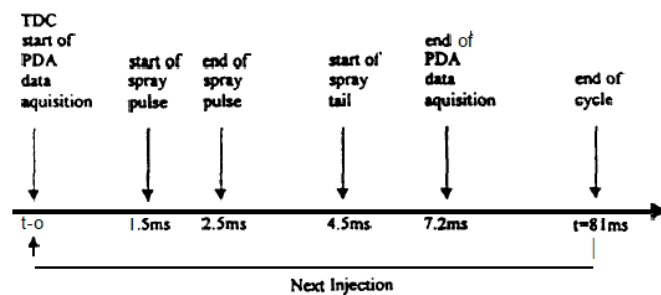


Fig 2. Data acquisition sequence for PDA.

PDA Technique:

The radius, speed, and reaching the time of droplets traveling through certain places in the spray were measured using Phase Doppler Anemometry (PDA). A 514.6nm Ar laser (ion) was employed with a DSC PDA system. The wind tunnel geometry required the 30° scattering angle, yet it measured the droplet diameter range properly. The software gave the size (0µm to 50µm) and axial velocity(-34m/s to + 119m/s)and ,the size (0µm to 50µm) for the measurement volume diameter of 74µm. The optics' photomultipliers that got the signal were merged to a DS software running computer and a processor

(signal) while Flow Measurement Consultancy Services' Insight software was used for more extensive analysis. The lenses (both sending and collecting) were placed on separate x,y,z systems(traverse), with each plane moving two hundred mm. The position inside the spray was defined using dial gauges with a 0.1 mm accuracy. The time gap in the PDA trigger data acquisition and the needle valve opening was checked to ensure that there was no substantial cyclic variation. A CCD video frame grabber device with an Ar light s (1 μ s) was used to get shadowgraphs of the sprays in normal situations.

Experimental Design:

At 3 points near the axis from the tip of the nozzle ($z=15,25,35$ mm), a PDA experiment was done and multiple radial places to provide a broad view of the spray structure, as shown in Figure III. Under cross-flow situations, the axis of the spray and the axis of the injector was not coincident. In quiescent conditions, the fluid mechanical spray axis and the axis of the injector were not coincident. As a result, prior to taking measurements, it was impossible to assume an evident spray center-line. By sending the beams at their crossover via a 100 μ m hole positioned along with the injector axis mounting in the tunnel. Standard reference position was determined. The spatial position $z=25$ mm, $r=0.0$ mm was established using a hole 25mm from the nozzle hole. At various points in the spray, PDA data of the 3 diesel were obtained (indicated in Figure III). The large density of the spray necessitated the mean of all the phases of numerous spray pulses, as with all diesel spray measurements. Two hundred sequential injections were done, with two hundred to two hundred fifty droplets monitored each injection over the beginning six milliseconds from the start. The data set may suffer from poor repeatability as a result of these techniques. To produce a measure of experimental repeatability, up to three replicate data were obtained at different times for most places. (Repeat data for the cross-flow situation were acquired exclusively for the diesel and diesel + additive cases.)

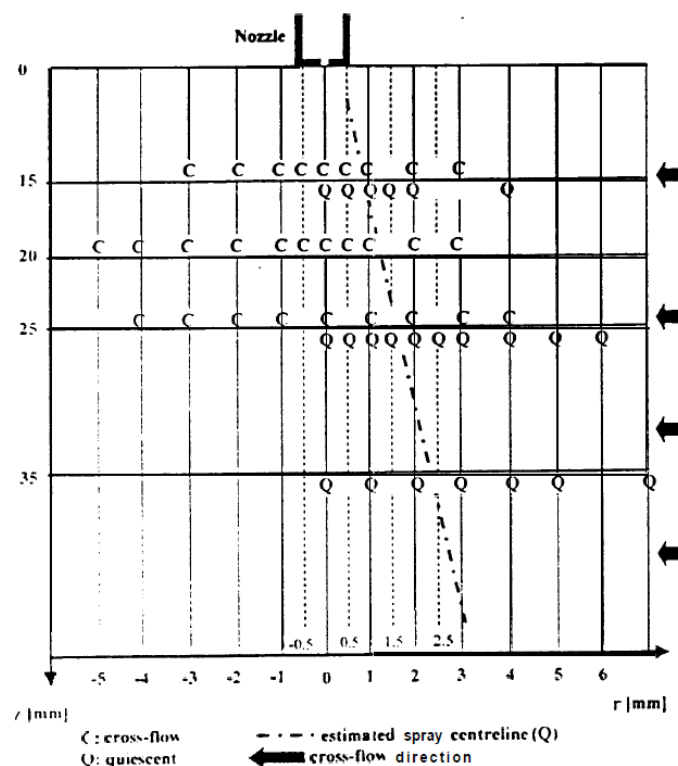


Fig 3 Measurement positions.

Experimental setup 2:

Visualization and Droplet Measuring System.

A visualization system was constructed to examine the injected spray diesel's characteristics and DME fuels as well as biodiesel, as shown in Figure 4a. The spray features were studied using spray pictures of several fuels under comparable injection settings to determine the spray formation process and axial as well as radial distances including spray cone angle. Last but not least, the spray area. A Nd:YAG laser, a cylindrical lens set containing a mirror, also a pulse generator (digital delay), an intensified charged coupled device camera, and a computer which is to act as an image grabber containing the spray visualization system used. The wavelength of source of light was 532 nm Nd: YAG laser. The spray evolution was illuminated using cylindrical lenses that created a laser beam (sheet) at most one millimeter thick. The spray picture was captured using a high-resolution ICCD camera. The droplet measurement device was used to look at tiny spray properties. The droplet size-frequency distribution, SMD, and mean velocity of the droplets were also measured. The droplet measurement system included a signal analyzer transmitter, and receiver as well as a photomultiplier tube and an Ar-ion laser with a power rating of 0.6W laser output. Output of photomultiplier tube and argon-ion laser voltage were tuned for the data rate r and intensity of the signal of the signal analyzer. The signal analyzer was synced with an injector driver using a digital delay/pulse generator to get time-resolved data. Table 1 lists the parameters for the spray visualization system and the droplet measurement system.

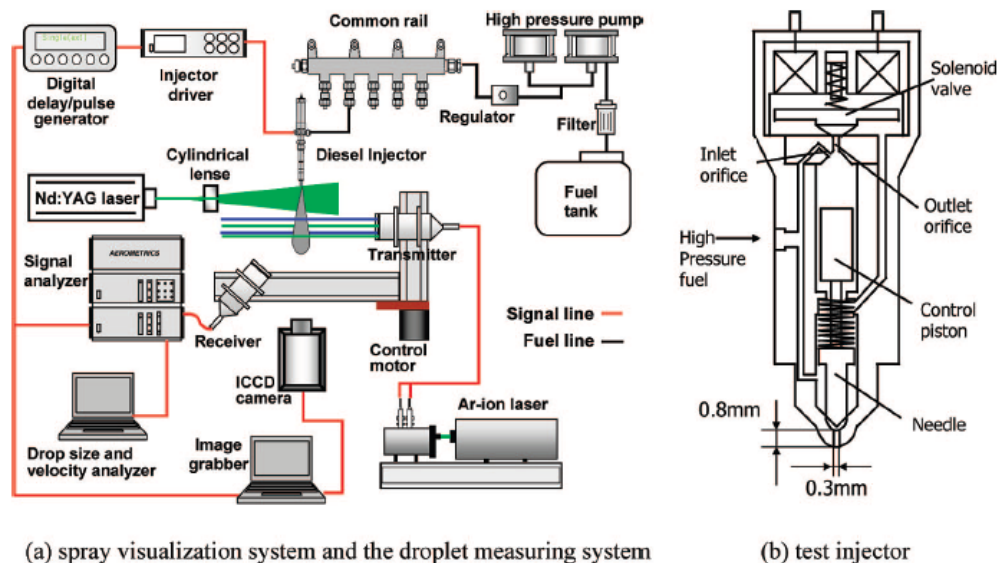


Fig 4. . Schematics of the experimental apparatus and test injector.

Experimental Procedures

The breakdown properties of the injection system (Common-Rail) were investigated using normal diesel or biodiesel. The parameters of testing fuel are provided in Table 2. The fuels that were inserted individually at a pressure of 60 Mega Pascal and 0.7 ms were required for energizing to investigate atomization properties. The diesel injector utilized in this study featured one hole with a 0.3 millimeter diameter of the nozzle and a ratio of 2.6 length/diameter as shown in Figure 4b. The tests on droplet measurement and visualization were carried out under ambient circumstances, which included a 0.1 MPa ambient pressure and a 293 K ambient temperature. Because the nozzle diameter was 300 μm , the subrange of diameter was adjusted from 3 μm to 79 μm , and about twenty thousand droplets were gathered and aggregated at every point of measurement. Including every ten mm (from five to thirty mm), the size of the droplet, as well as velocity were noted.

Table 2(a): Specifications of Visualization Systems

light source	Nd:YAG laser
laser power (mJ)	maximum of 270
wavelength (nm)	532
beam thickness (mm)	~1
resolution	1280 (height) x 1024 (vertical)

Table 2(b): Specifications of Droplet Measuring Systems

light source	Ar-ion laser
wavelength (nm)	514.5, 488
laser beam diameter (mm)	1.4
beam expand ratio	0.5
focal length (transmitter) (mm)	500
focal length (receiver) (mm)	250
collection angle (deg)	30
filter frequency (MHz)	40
PMT voltage (V)	500
diameter subrange (μm)	2-80
velocity subrange (m/s)	from -292 to 292

Table 3. Properties of the Test Fuels

Fuel properties	diesel	biodiesel (soybean oil)	DME (dimethyl ether)
carbon content (wt %)	87	77	52
hydrogen content (wt %)	13	12	13
oxygen content (wt %)	0	11	35
density (kg/m ³)	828	884	660
viscosity (mm ² /s)	2.835	4.022	0.12 - 0.15
Surface tension (kg/s ²)	0.027	0.028	0.012
boiling point temperature (°C)	180 - 340	315 - 350	-23
flash point temperature (°C)	60 - 80	100 - 170	-42
cetane number	40 - 55	48-63	68

Results and Discussion:

Experiment 1:

PDA measurements (Quiescent Conditions)

Pulse data (Overall):

To get an overall assessment, Figure 5 shows the fluctuation in droplet size as a function of spray position (the droplet size is calculated using the formula defined as $SMD = \sum N_i D_i^3 / \sum N_i D_i^2$). The following observations can be made based on the outcomes of all the test runs that satisfied the criteria:

1. There were only minor differences in "overall" droplet size as a function of radial position. This is in line with previous research [8], which found that droplet size is not dependent on the radial position inside the spray.
2. The dissimilarities in the fuels were clearly noticeable at the periphery. The droplet sizes of diesel/kerosene may be smaller.
3. On repeat runs, the variability was so high that only variations of 3µm or more amongst fuels could be regarded as significant.

4. Fuel seemed to have no effect on the total size of the droplets in these studies

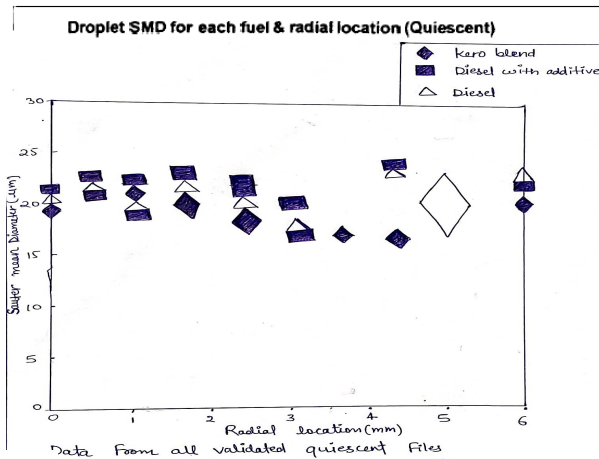


Fig 5. Sauter Mean Diameters for complete 6ms spray interval versus radial position.

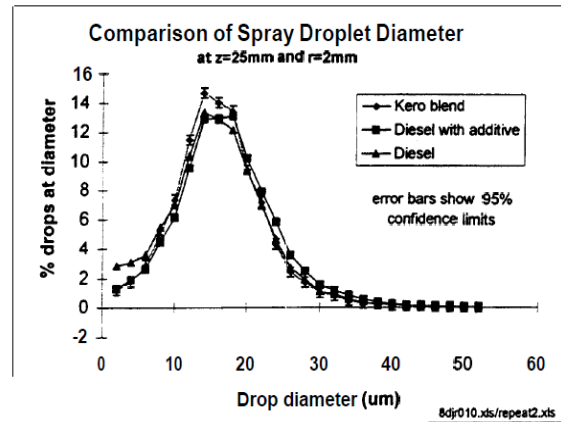


Fig 6. Overall drop size distributions at z=25mm, r=2mm, quiescent gas.

Figure 6 depicts the distribution of diameter of droplet around the fluid mechanical center-line at radius=two mm and axial location of z=twenty mm,(For diesel fuel, there was only one certified test point available.) The findings reveal that droplet size changes were minimal (about 15%) and that the fuel had not caused a significant shift in the diameter distribution. However, when the sprays had reached up to z=25mm, video shadowgraphs revealed that there was a difference in angles for the particular diesel compared. Although more data is needed to corroborate this, the new diesel fuel has a thinner spray (c. 19% smaller angle) than either fuel. This was noticed when shifting the measurement volume, as droplet data for the additised diesel could be gathered over a narrower radial region than for the other two fuels.

Time-resolved data:

It should be noticed that both pictures in the figure are time-averaged of the spray from the previous section. For the three fuels, Figure 7 depicts scatter diagrams of velocities of droplets around the radial centers at 14.5mm downstream. Near the front border of the spraying pulse, these velocity-time records show the predicted fast spike in velocity. The tiny negative velocity prior to the spraying pulse is caused by a backflow of air as it recirculates inside the chamber. In the tail, the slow decline of the velocity of the spraying pulse is plainly seen. The graph also includes solid lines that represent data rate time histories (arbitrary scales). In the middle of the spray pulse the value of the data is quite low, despite the fact that the rates for the new diesel are greater than diesel and 50% mixture of kerosene. Figure 8 depicts the graph of velocity and numerical average diameter time, as well as 14.5 mm downstream. Figure 8 (b) should be interpreted with caution since the size of the drop is around 2ms corresponding to droplets present in the gas. At this location, the average diameters of the fuels are within 2 μ m of one another, despite the varied arrival timings.

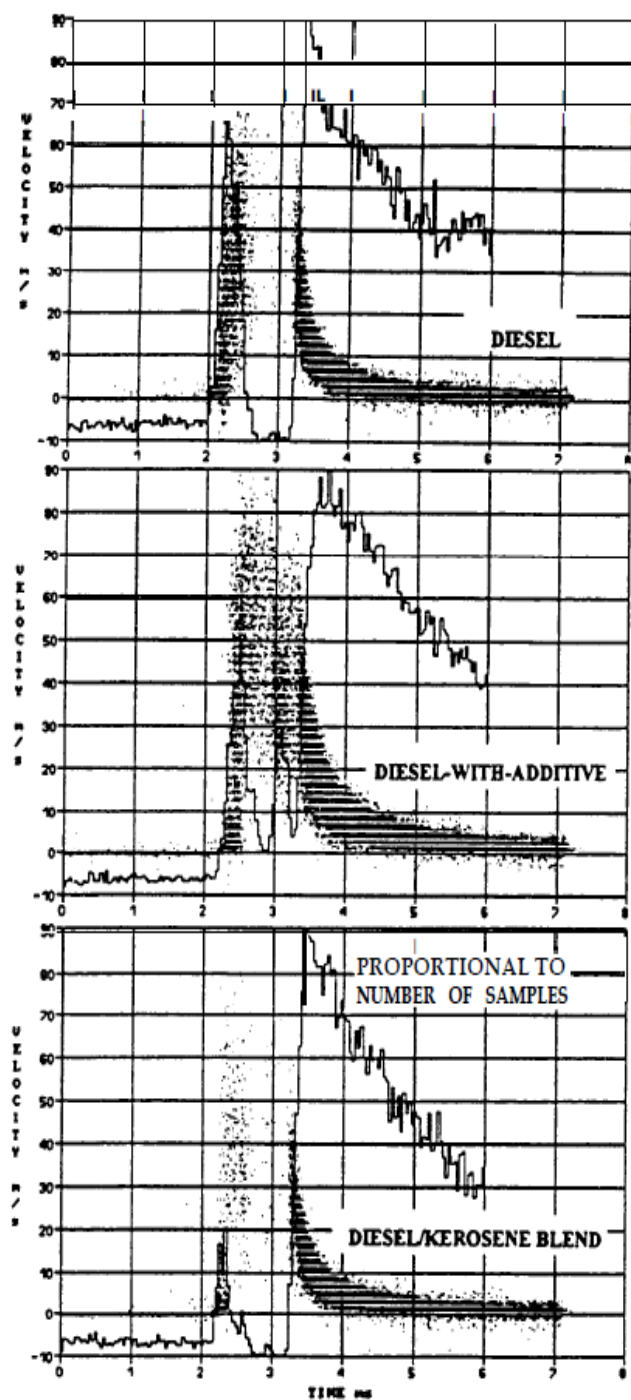


Fig 7. Drop velocities at $z=15\text{mm}$, $r=1\text{ mm}$, for three fuels, quiescent gas.

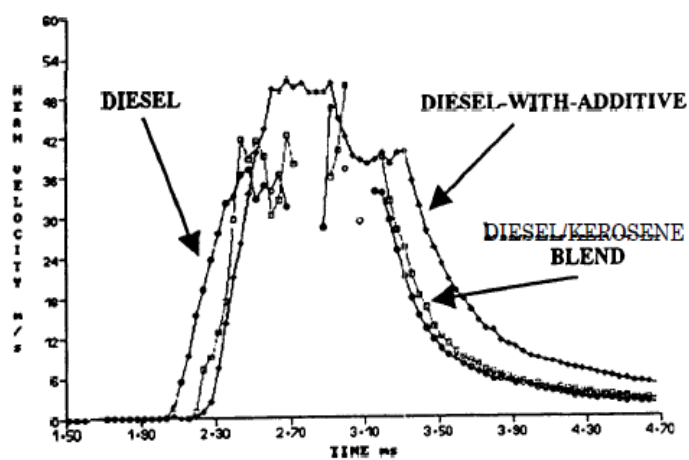


Fig 8 (a) Example Mean Velocity-Time histories, $z=15\text{mm}$, $r=1\text{ mm}$, quiescent gas.

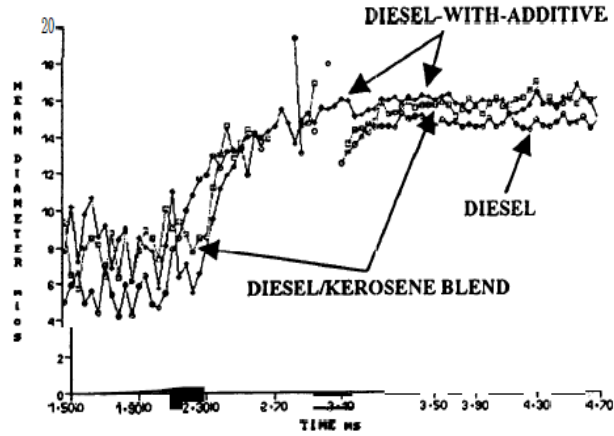


Fig 8(b) Numerical Mean Diameter-Time histories,
 $z=15\text{mm}$, $r=1\text{mm}$, quiescent gas.

Figure 9 demonstrates the sets of velocity-time graphs for the three fuels for $z=25\text{mm}$ and $r=1\text{mm}$, $r=2.5\text{mm}$, and $r=6\text{mm}$. The graphic contains repeat testing to show the data's repeatability. The findings for all fuels are comparable, as can be shown. The primary spray pulse area should be used to make comparisons. The comparable numerical mean drop diameter histories are shown in Figure 10. The duration of the tail, the primary spray pulse, and the preceding gas areas are all recorded in one data set (obtained by looking at the associated velocity history). The sizes of the droplets are smallest at the edge of the primary spray pulse ($\approx 6\text{-}8\text{ }\mu\text{m}$ mean diameter), and the biggest droplets are occurring at the trailing edge ($\approx 13\text{-}16\text{ }\mu\text{m}$ mean diameter). In comparison to the SMD shown in Figure 5, these are the numerical mean diameters of the droplet. The variations between the fuels in Figures 9 and 10 are relatively less. When looking at the arrival timings of the major spray pulses (at radius $=1\text{mm}$ and radius $=3\text{ mm}$; Fig 9) the times customized diesel (with additives) fuels and for the diesel are comparable, but the mix sprays of kerosene and diesel blend come one-tenth millisecond later. The constancy of discrepancies at radial positions concludes the idea that different fuels have distinct impacts.

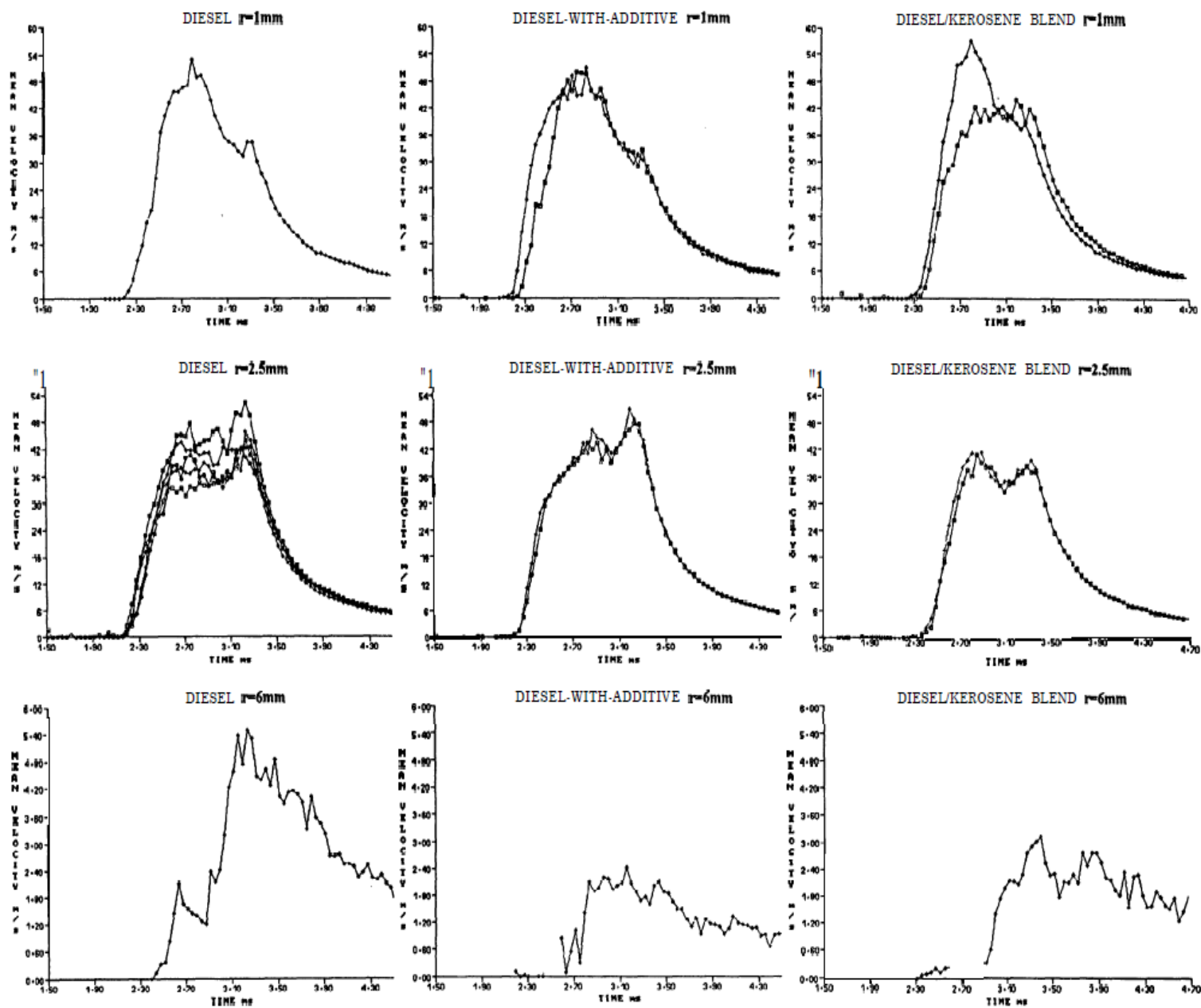


Fig 9 Velocity-Time histories showing all repeat data at $z=25\text{mm}$, quiescent

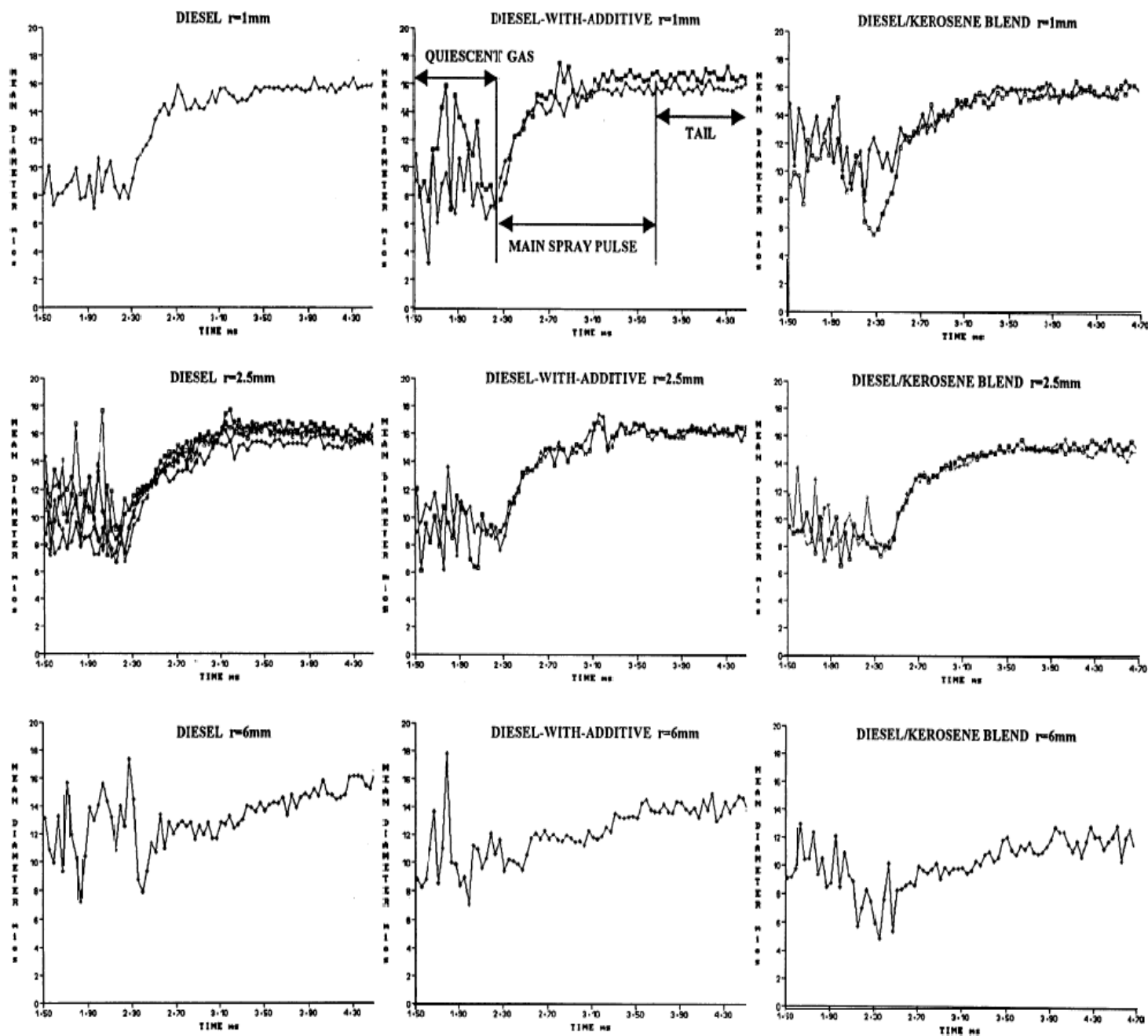


Fig 10 Droplet Size-Time histories showing all repeat data at $z=25\text{mm}$, quiescent

PDA measurements - Crossflow:

One test per fuel yielded validated data sets under cross-flow circumstances. As a result, no conclusive conclusions concerning fuel impacts can be formed because the magnitude of such effects cannot be assessed.

Spray pulse data:

The droplet size distribution is shown in Figure 11 at two mm upward of the inserter axis. The fuel droplet distribution appeared to be more distinct under cross-flow conditions; this was due to the elimination of droplets before, leaving data indicative of the core of the spray. These findings show that the kerosene mix created a greater number of extremely tiny droplets.

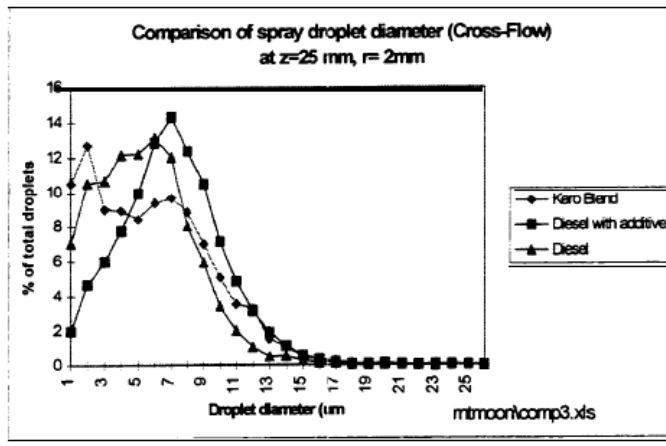


Fig 11 Overall (7ms averaging window) drop diameter distributions at $z=25\text{mm}$, $r=2\text{mm}$, with cross-flow.

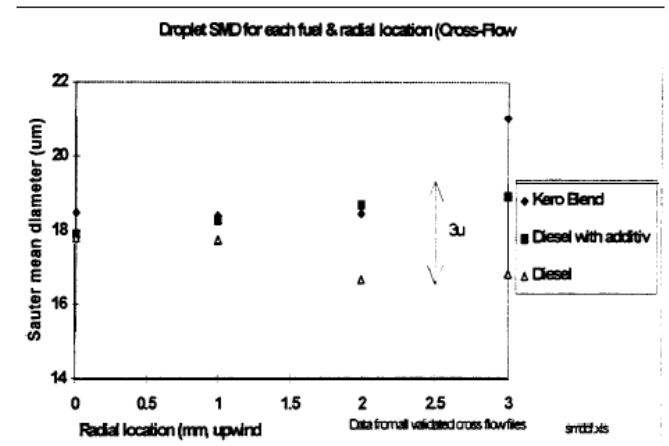


Fig 12 Overall (7ms averaging window) Sauter Mean Diameter at $z=25\text{mm}$.

In Figure 12, when size of droplet is plotted versus location in spray, a distinct pattern emerges. The findings show that the kero mix had the largest average size near the spray's edge ($r = 3\text{mm}$, upwind). This reason is thought to be the cross-wind that blew a higher proportion, resulting in an SMD that was relatively big in comparison to the other fuels. The trendline formed between the points indicates that the data are most likely depicting a true impact.

Time-Resolved Data:

At radius = three mm (i.e. upstream) and $z=20\text{mm}$, Figure 13 displays speed scatter graphs for the fuels. The diesel has greater speed than the rest of the fuels, as shown by a higher number and faster arrival time. According to the video shadowgraphs, these measurements are predicted from a spray that suffers little deflection than the rest. The mean droplet diameter for the diesel case tended to be slightly higher (up to two μm higher numerical means diameter) for most positions in the sprays than for the

diesel or kerosene blend, as shown in Figure 14, shows numerical average diameter time for the same data.

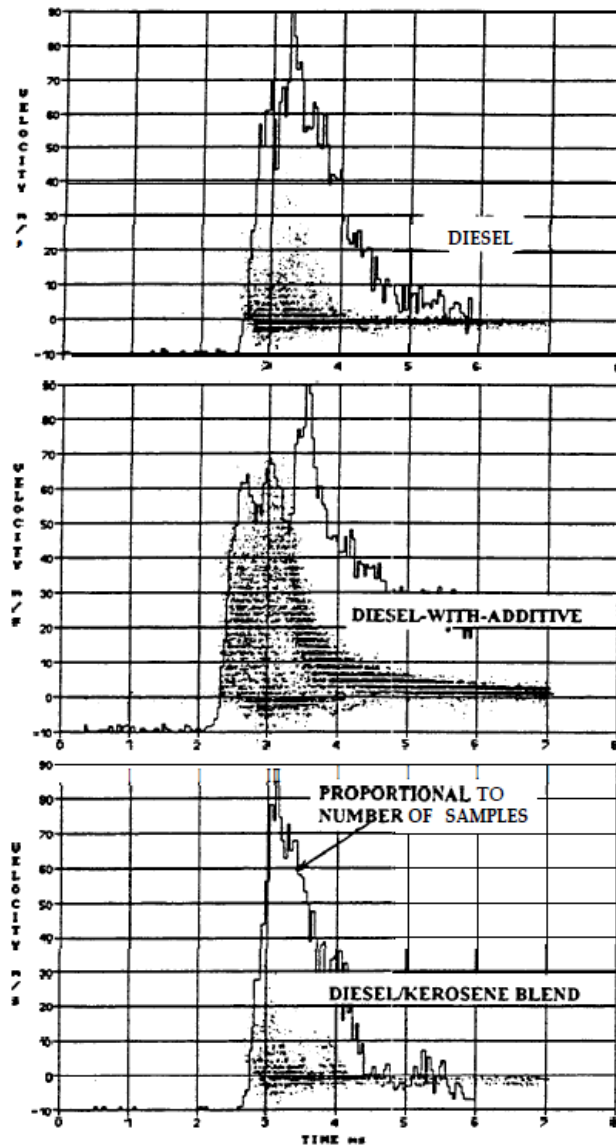


Fig 13 Velocity at $z=25\text{mm}$, $r=3\text{mm}$, with cross-flow.

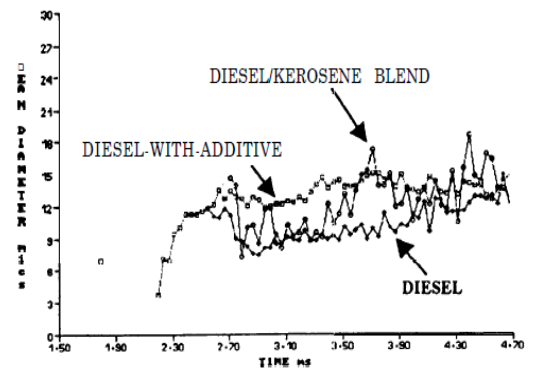


Fig 14 Mean Diameter-Time histories at $z=25\text{mm}$, $r=3\text{mm}$, with cross-flow.

Experiment 2:

Droplets on axial distances in the range of five to thirty millimeters from the starting of the nozzle were calculated using Phase Doppler Particle Analyzer to examine the atomization properties based on the distance of the axis from the nozzle. The axial distance's impact on the frequency curves of three fuels in ascending order of fuel size is shown in Figure 15. As the distance from the axis of the tip rises, the gradient of curves of droplets with diameters of fifteen μm becomes steeper. Many tiny droplets having diameters less than fifteen μm were dispersed, although these droplets had a narrow distribution at the nozzle tip. Furthermore, when the droplet diameter was between 10 μm and 15 μm , the order of curves is reversed for the fuels, defining the cross points shown in Figure 15. As shown in Figure 15b, the curves of biodiesel in accordance with the distance from the axis are comparable to those of the other two fuels. Due to the large surface tension and viscosity, the atomization of biodiesel spray advances slowly until the axial distance reaches 35 mm, according to this finding. At axial distances of twenty and thirty mm, the frequency distributions of DME spray exhibit almost identical curves to those shown in Figure 15c. Because of the volatile properties of DME fuel, numerous droplets whose size is smaller than 10 μm evaporated at a distance of thirty mm from the axis.

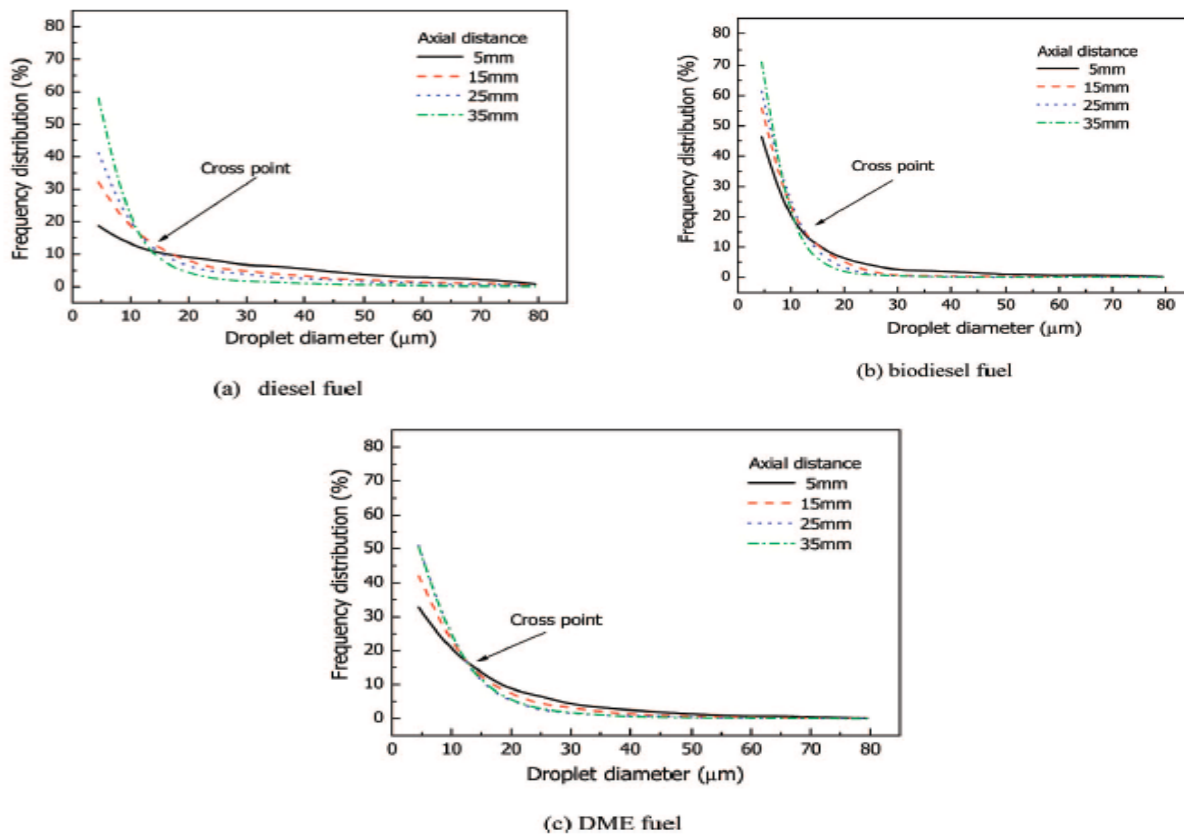


Fig 15 . Effect of the axial distance on the distribution ratio curves of the three fuels according to the droplet size.

Figure 16 shows the impact of the distance from tip of the nozzle from the axis on SMD as a time's function since the insertion began. With the increase in distance from the tip , SMD values of the fuels are decreases. Also, the droplet after the insertion has produced collisions of inserted droplets, the SMD in accordance with the distance rose as time passed from the commencement of the insertion. Biodiesel has a viscosity more than diesel, the growth of SMD in biodiesel is faster. Biodiesel and diesel fuels have an SMD range of 30-70 meters, whereas DME fuel has an SMD range of 10-40 meters. Because of its increased volatility and lower density, the show of DME is better than both the fuel, according to these findings.

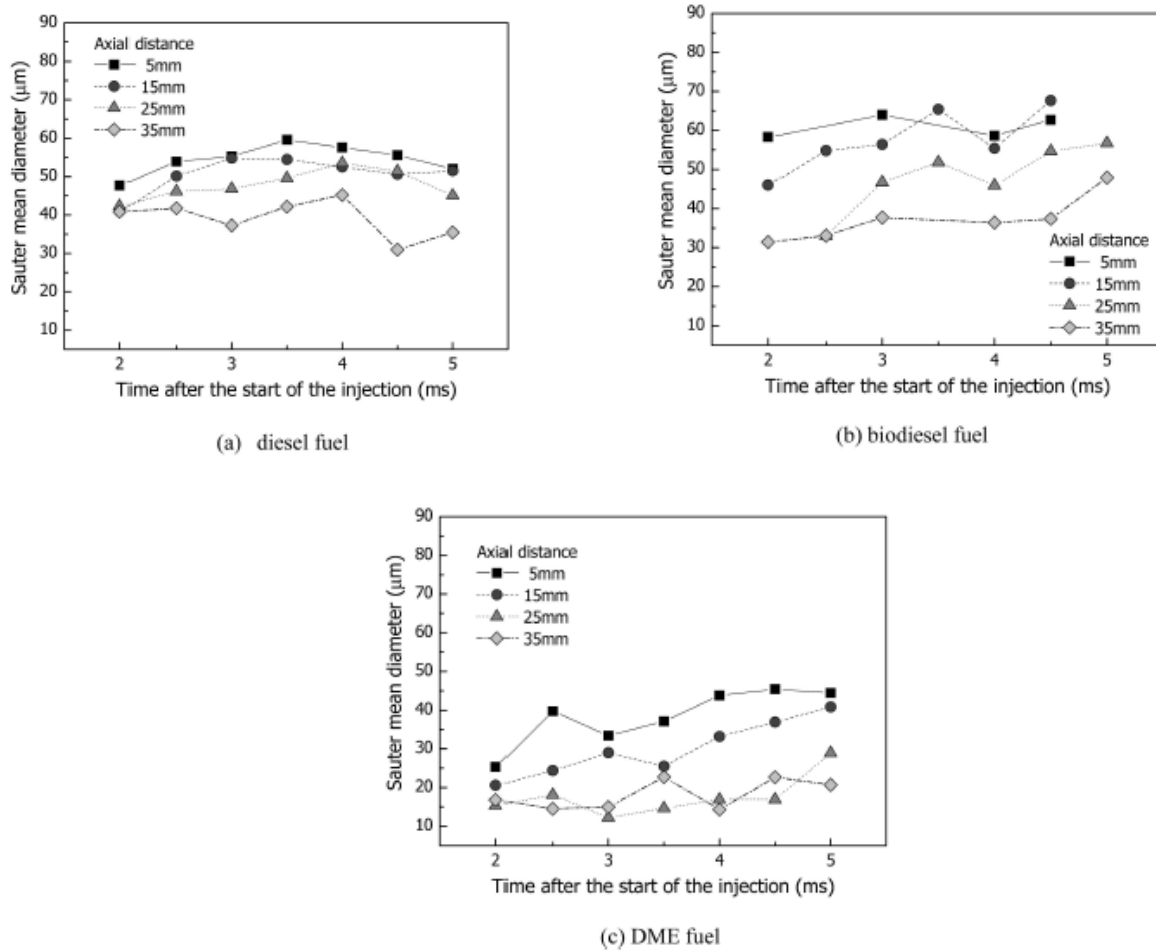


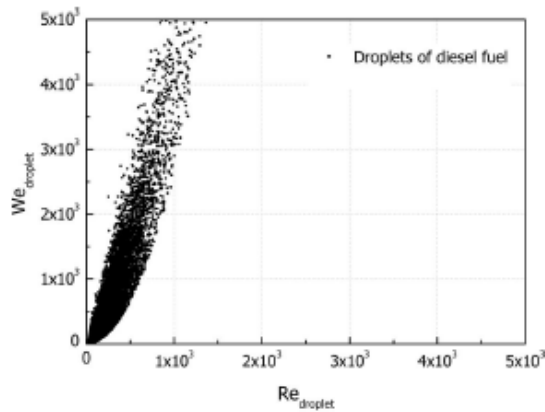
Fig 16 . Effect of the axial distance from the nozzle tip on the SMD according to the time after the start of the injection.

Figure 17 shows the relationship between Reynolds and Weber's numbers for the fuels. The droplet Weber and Reynolds numbers were computed using the velocity, diameter, density, and surface tension of droplets at twenty degrees centigrade, according to fuels, as described:

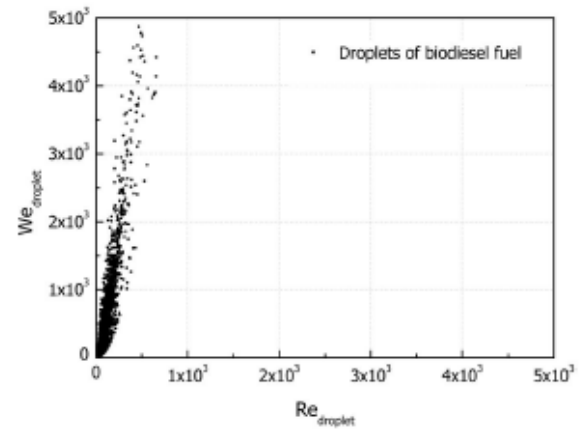
$$We_{\text{droplet}} = \frac{\rho_{\text{fuel}} U_{\text{droplet}}^2 D_{\text{droplet}}}{\sigma_{\text{fuel}}}, \quad Re_{\text{droplet}} = \frac{\rho_{\text{fuel}} U_{\text{droplet}} D_{\text{droplet}}}{\mu_{\text{fuel}}}$$

The average speed of droplets was derived from the radial velocity and also axial to estimate the We and Re of droplets. The droplet was impacted by surface tension and viscosity when Reynolds and Weber numbers were compared.

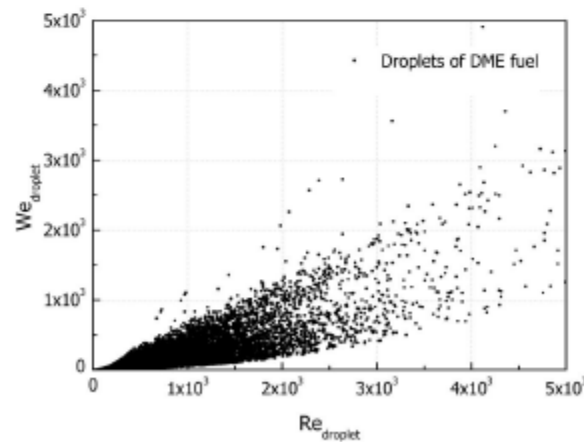
The droplets' We and Re values were also enhanced due to their rapid velocity and big size. The viscosity, rather than the velocity. In comparison to DME fuel, biodiesel's gradient along with viscosity has a sharp slope as well as a limited breadth. Since DME fuel has low viscosity, the Reynolds number increases at a faster pace than the Weber number, the gradient of DME has neither too high nor too low slope, as illustrated in Figure 17c. Furthermore, due to the low viscosity of DME fuel possesses a greater Re , but biodiesel with a greater viscosity possesses a lower Re . High surface tension causes biodiesel and diesel fuels to have high values when compared to DME. From this, we predict that the Weber number of droplets impacted the factor, but that the Reynolds number also has a significant impact on the primary breakup factor.



(a) diesel fuel



(b) biodiesel fuel



(c) DME fuel

Fig 17. Relation between the Weber and Reynolds numbers for the three fuels.

Conclusion:

From experiment 1:

Discussion:

The three fuels had less influence on the size of the droplet, with variances of less than $3\mu\text{m}$ (15 percent) according to PDA data taken under quiescent circumstances. The cross-flow circumstances enabled for a larger proportion of droplets to be measured in the spray's high density body. This indicated that the kerosene mix created a greater quantity of extremely minute droplets. The spray cone might potentially be seen using time-resolved data (Though the data has variations). As demonstrated by the later arrival timings, the kerosene blend diesel has less penetration. The additized diesel spray, on the other hand, exhibited a greater velocity and narrower spray under time-resolved circumstances, as seen by the video shadowgraphs. In light of studies [7], the thinner, spray with more penetration for additized diesel fuel might be considered. Similar research found that a gasoline treated with the same additive vaporised less, as evaluated by two separate methodologies (Exciplex and laser diffraction). This is in line with the fact that reduced volatility fuels may reach the combustion chamber more deeply.[15,16].

The following conclusions can be drawn.

(i) There was no significant effect on the size of the droplet due to the change in fuels. However, it had a certain impact on the spray structure. A narrow spray (cone angle lesser than 20%) was observed in the diesel-with additive fuel than the diesel or the diesel blended with kerosene.

This is in line with the study [18] viscosity, bulk modulus and density has a combined effect on the spray tip penetration measurement.

(ii) Certain results indicate that narrow spray is produced when detergent is used as an additive in the diesel fuel.

It is in line with the study. [17] Results show that the spray development process (spray cone angle and tip penetration) is affected by viscosity and to some extent fuel density.

From experiment 2 :

(i) The breakdown factor of diesel fuels and bio diesel was impacted by the Weber number of droplets when the Reynolds and Weber numbers of droplets were compared. Since DME fuel has low viscosity, the Reynolds number increases at a faster pace than the Weber number. Meanwhile, the major breakdown factor of the DME fuel was heavily influenced by the Reynolds number of droplets.

Similar results in studies [17] stated a change in surface tension from 18 to 30 mN/m had no discernible effect on spray properties. The narrow range of change in surface tension, as well as the comparatively high Weber number under diesel-like circumstances, might explain this.

(ii) with the increase of the distance from the axis and the tip of the nozzle, the SMD of the diesel, biodiesel, and DME fuels is reduced.

(iii) Biodiesel and diesel fuels have an SMD range of 30-70 metres, whereas DME fuel has an SMD range of 10-40 metres. Due to DME fuel's lower density and increased volatility, its atomization performance is superior than that of diesel fuels as well as bio diesel, according to these findings

Combining the results from the above experiments we conclude that in general changing of diesel fuel or using additive or biodiesel(as it is closely related to diesel) there is no significant change in droplet size thus atomization characteristics are not affected much however DME fuel has better atomization. Also, we conclude that change in fuel can bring about change in the spray cone structure. Several studies as indicated above also suggest the same however we do realize that experimental conditions and set up were different for different cases. The study [19] however gave a different result. " spray penetration and cone angle do not change significantly with fuel type" which can be due to change in experimental conditions. For improvement purposes if we could test more number of times (limited data samples) as there might be little change in droplet size which is not detected while performing the experiment.

Reference:

- [1] Reitz, RD and Bracco, FV. On the dependence of spray angle and other spray parameters on nozzle design and operating conditions. SAE Paper 790494, 1979.
- [2] Elkotb, M-M. Fuel atomization for spray modeling. Prog Energy Combust Sci, 8, 61-91, 1982.
- [3] E. Giffen, A Muraszew. The Atomisation of Liquid Fuels Chapman & Hall, London (1953)
- [4] Desantes JM, Arregle, Pastor JV Delage A. Influence of the fuel characteristic on the injection process in a DI Diesel Engine, SAE paper 980802, (1998)
- [5] The European programme on Emissions, Fuels and Engine Technologies (EPEFE) Europa/ACEA, 1995
- [6] Yule, AJ and Aval, SM. A technique for velocity measurement in diesel sprays. Combustion and Flame, 77, 385-394, 1989.
- [7] Pan, G. A study of the influence of fuel additives on atomization and evaporation of diesel fuel. MSc Thesis, Dept Mech and Aerospace Eng, Princeton Univ, June 1996.
- [8] Payri F, Desantes JM, Arregle J; Characterisation of DI Sprays in High Density Conditions, SAE paper 960774, (1996)
- [9] Pitcher, G and Wigley, G. The droplet dynamics of diesel fuel sprays under ambient and engine conditions. Proc ASME Conf Laser Anemometry, 2, 571-586, 1991.
- [10] Behrouz, C. Preliminary drop size and velocity measurement in dense diesel type sprays. SAE Paper 901673, 1990.
- [11] Reitz RD, Diwakar R; Structure of High-Pressure Fuel Sprays, SAE Paper 870598 (1987).
- [12] Tanner FX; Liquid Jet Atomisation and Droplet Breakup Modeling of Non-evaporating Diesel Fuel Sprays, SAE Paper 970050 (1997)
- [13] Liu AB, Mather D, Reitz RD; Modeling the Effects of Drop Drag and Breakup on Fuel Sprays, SAE Paper 930072 (1993)

- [14] Hohmann S, Klingsporn M, Renz U; An improved Model to describe Spray Evaporation under Diesel-like conditions, SAE paper 960630 (1996)
- [15] Siebers DL; Liquid-Phase Fuel Penetration in Diesel Sprays, SAE paper 980809 (1998)
- [16] Canaan RE, Dee JE, Green RM, Daly DT; The influence of Fuel Volatility on the Liquid-Phase Fuel Penetration in a Heavy-Duty DI Diesel Engine, SAE paper 980510 (1998).
- [17] J. Dernotte, C. Hespel, S. Houill'e, F. Foucher & C. Mouna'im-Rousselle, Influence Of Fuel Properties On The Diesel Injection Process in Non Vaporizing Conditions Atomization and Sprays, 22 (6): 461–492 (2012).
- [18] Pin-Chia Chen , Wei-Cheng Wang , William L. Roberts , Tiegang Fang . Spray and atomization of diesel fuel and its alternatives from a single-hole injector using a common rail fuel injection system. Fuel 103 (2013) 850–861.
- [19] L. C. Goldsworthy, C. Bong, & P. A. Brandner. Measurements of Diesel spray Dynamics And The Influence Of Fuel Viscosity Using PIV and Shadowgraphy Atomization and Sprays, 21 (2): 167–178 (2011).